

Article

SUPPORTING INFORMATION

Low-Carbon Composite Based on MOC, Silica Sand and Ground Porcelain Insulator Waste

Adam Pivák ¹, Milena Pavlíková ¹, Martina Záleská¹, Michal Lojka², Anna-Marie Lauermannová², Ondřej Jankovský² and Zbyšek Pavlík ^{1,*}

¹ Department of Materials Engineering and Chemistry, Faculty of Civil Engineering, Czech Technical University in Prague, Thákurova 7, 166 29 Prague 6, Czech Republic; adam.pivak@fsv.cvut.cz (A.P.); milena.pavlikova@fsv.cvut.cz (M.P.); martina.zaleska@fsv.cvut.cz (M.Z.)

² Department of Inorganic Chemistry, Faculty of Chemical Technology, University of Chemistry and Technology Prague, Technická 5, 166 28 Prague 6, Czech Republic; michal.lojka@vscht.cz (M.L.); lauermaa@vscht.cz (A.-M.L.); ondrej.jankovsky@vscht.cz (O.J.)

* Correspondence: pavlikz@fsv.cvut.cz; Tel.: +42-0224-354-731

Received: 2 July 2020; Accepted: 10 July 2020; Published: 13 July 2020

2. Experimental Methods

The chemical composition of quartz sand, PW, and commercially delivered MgO were tested on XRF (X-Ray fluorescence) principle using an ED-XRF spectrometer ARL QUANT'X (Thermo Scientific). The software UniQuant 5 (Thermo Scientific) was used to collect and analyze the measured data. The typical dry sample mass was 7–10 g.

X-ray powder diffraction (XRD) data of PW were collected at room temperature on a Bruker D8 Discoverer powder diffractometer with parafocusing Bragg–Brentano geometry using CuK α radiation ($k = 0.15418$ nm, $U = 40$ kV, $I = 40$ mA). Data were scanned over the angular range 5–80° (2θ) with a step size of 0.019° (2θ). Data evaluation was performed in the software package HighScorePlus.

The morphology was investigated using scanning electron microscopy (SEM) with a FEG electron source (Tescan Lyra dual beam microscope). Elemental composition and mapping were performed using an energy dispersive spectroscopy (EDS) analyzer (X-MaxN) with a 20 mm² SDD detector (Oxford instruments) and AZtecEnergy software. To conduct the measurements, the samples were placed on a carbon conductive tape. SEM and SEM-EDS measurements were carried out using a 10 kV electron beam.

Specific density, loose bulk density, and Blaine fineness of MgO, silica sand, and PW were also tested. For the specific density assessment, an automatic helium pycnometer Pycnomatic ATC (Porotec, Hofheim, Germany) was used. The loose bulk density was calculated based on the dry mass of the sample in a graduated cylinder. The Blaine fineness of MgO and PW was measured in compliance with the technical standard EN 196-6.

The particle size distribution of PW was analyzed by an Analysette 22 Micro Tec plus (Fritsch GmbH) device with two semiconductor lasers, green ($\lambda = 532$ nm, 7 mW) and IR ($\lambda = 940$ nm, 9 mW), was used. The apparatus operates on a laser diffraction principle. PW was measured 5 times (5 scans) and particle size distribution curves were created from the average values.

The grain size distribution of silica sand was determined in the standard sieve test conducted in accordance with the EN 933-1.

The workability of fresh mixtures was verified using a flow table test which was realized in compliance with the EN 1015-3.

The hardened composites were tested after 28 days of maturing under laboratory conditions. For the hardened materials, phase composition, structural parameters, water transport and storage

properties, and thermo-physical properties were examined. The simultaneous thermal analysis (STA) of the matured materials and their FT-IR analysis were also conducted.

Phase composition was tested on MOC/PW pastes only as the silica peaks would overlap the XRD peaks of precipitated MOC phases. X-ray powder diffraction of MOC/PW pastes was performed similarly as in analysis of PW.

The investigated structural parameters of MOC composites were bulk density, specific density, and porosity. For each composite, minimally 5 samples were tested. The dry bulk density ρ_b ($\text{kg}\cdot\text{m}^{-3}$) was determined according to the standard EN 1015-10 with the expanded combined uncertainty of 1.4 %. The specific density ρ_s ($\text{kg}\cdot\text{m}^{-3}$) was measured by helium pycnometry (see above). The typical dry sample mass was about 40 g. The samples were dried at 60 °C in a vacuum dryer VacuCell (BMT, Brno, Czech Republic). The expanded combined uncertainty of the specific density test was 1.2 %. Based on the bulk density and specific density data, the porosity φ (%) was calculated. The expanded combined uncertainty of the porosity assessment was 2.0 %.

The mechanical resistance of investigated composites was characterized in flexural strength, compressive strength, and dynamic modulus of elasticity tests. The strength tests were realized in accordance with the EN 1015-11 using a testing device EDB 400 (Heckert, Germany). The flexural strength R_f (MPa) was measured on standard prisms in three point bending test arrangement. The compressive strength R_c (MPa) was measured on the far edge of the specimen fragments from flexural strength testing. The loading area was 40 mm \times 40 mm. The expanded combined uncertainty of both strength tests was 1.4 %. The dynamic modulus of elasticity E_d (GPa) was assessed in the ultrasound velocity test using an instrument Pundit Lab+ (Proceq, Schwerzenbach, Switzerland) with a couple of 54 kHz transducers. The expanded combined uncertainty of this test was 2.3 %.

Mercury intrusion porosimetry was used for the detailed investigation of the pore structure of hardened composites. The analysis was done by the use of porosimeters of Pascal series, Pascal 140 and Pascal 440 (Thermo Fisher Scientific). Typical sample mass was \sim 1 g.

As reported in literature, the biggest lack of MOC-based materials is their susceptibility to moisture damage. Therefore, the hygric parameters of developed composites, namely water absorption coefficient, water sorptivity, apparent moisture diffusivity, and 24 h water absorption were determined. The water absorption coefficient A_w ($\text{kg}\cdot\text{m}^{-2}\cdot\text{s}^{-1/2}$) and water sorptivity S_w ($\text{m}\cdot\text{s}^{-1/2}$) were measured in the free water uptake experiment in accordance with the EN 10115-18. From the assessed A_w value and the maximum of the imbibition curve of water, the apparent moisture diffusivity κ_{app} ($\text{m}^2\cdot\text{s}^{-1}$) was calculated. The expanded combined uncertainties of the water absorption and sorptivity tests were 2.3 %, and that of the apparent moisture diffusivity test was 3.5 %. The 24 h water absorption W_a (%) was measured with the expanded combined uncertainty of 1.2 %. In this test, experimental procedure prescribed in the EN 772-11 was followed.

Among thermal parameters of composites, dry thermal conductivity λ ($\text{W}\cdot\text{m}^{-2}\cdot\text{K}^{-1}$), thermal diffusivity a ($\text{m}^2\cdot\text{s}^{-1}$), and volumetric heat capacity c_v ($\text{J}\cdot\text{m}^{-3}\cdot\text{K}^{-1}$) were tested. These parameters were determined by a transient plane source technique. Hot-disk thermal analyzer TPS 1500 (Hot Disk AB) with Kapton-insulated sensor was used. Tests were carried on dry samples at room temperature of (24 ± 1) °C.

Mid-infrared spectra of hardened MOC composites were collected with FT-IR Nicolet 6700 spectrometer (Thermo Fisher Scientific, Waltham, MA, USA) after 32 scans with wave numbers ranging from 4 000 to 400 cm^{-1} and with a spectral resolution of 4 cm^{-1} . Samples were firstly crushed and consequently powder was homogenized in an agate grinding mortar. The measurements were performed using ATR accessory with diamond crystal in absorbance mode. The automatic correction was used for final spectra presentation. The measured data was analyzed as a raw data firstly, without any automatic correction.

Thermal behavior of the prepared samples was analyzed by Simultaneous thermal analysis (STA). The DTA and TG curves were recorded simultaneously on a Linseis STA PT1600 apparatus at a heating rate of 5 °C \cdot min $^{-1}$ in a dynamic air atmosphere (50 mL \cdot min $^{-1}$).

Individual standards followed are listed in the Section 4.

3. Results and discussion

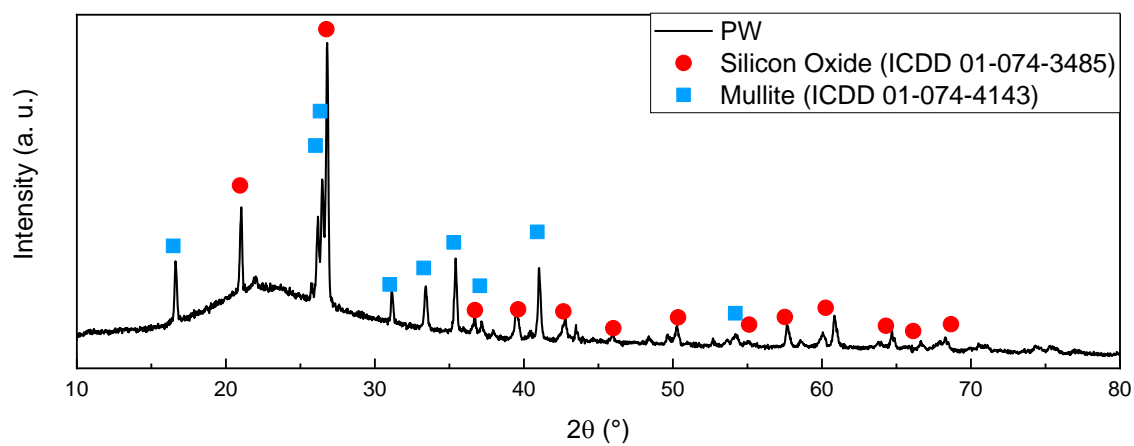


Figure S1. Diffraction pattern of PW.

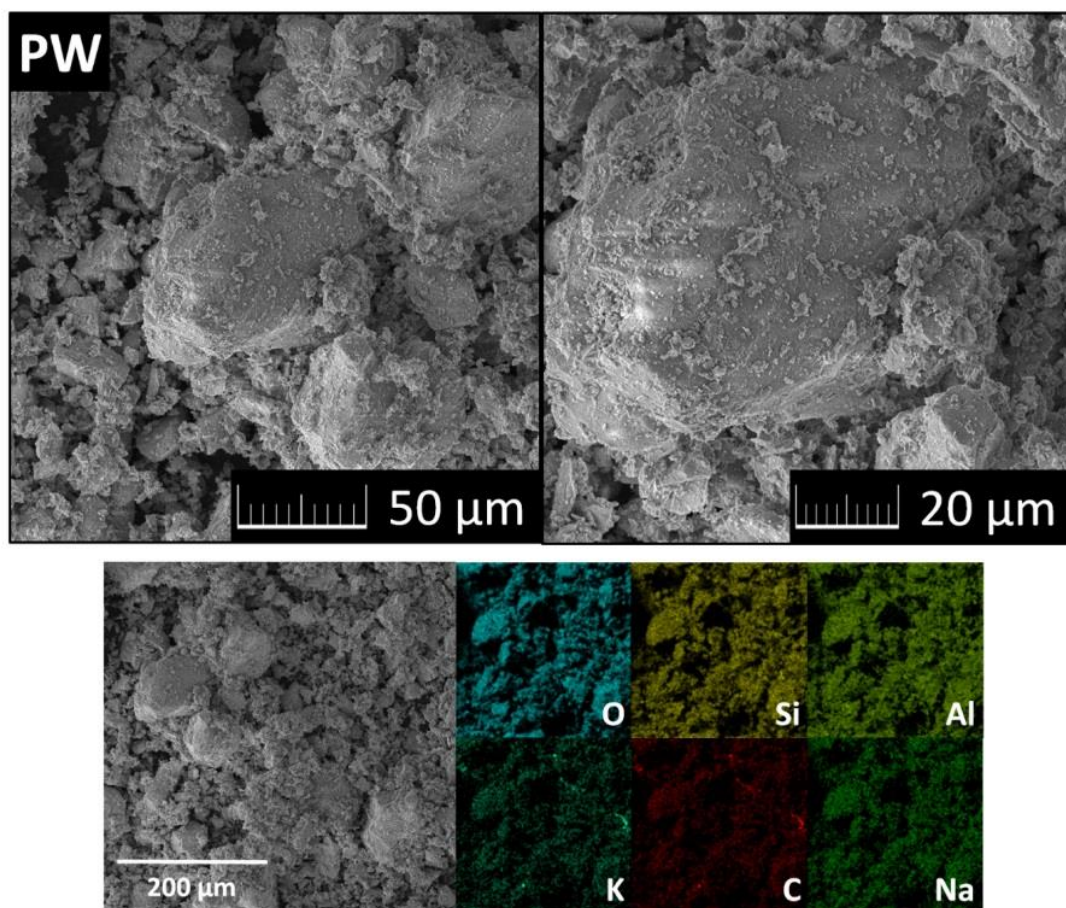


Figure S2. SEM micrographs with different magnifications and EDS element maps of PW.

4. Standards

1. EN 14016-2: Binders for Magnesite Screeds - Caustic Magnesia and Magnesium Chloride - Part 2: Test Methods; European Committee for Standardization: Brussels, Belgium, **2004**.
2. EN 196-6: Methods of Testing Cement. Determination of Fineness; European Committee for Standardization, Brussels, Belgium, 2018.
3. EN 933-1: Test for Geometrical Properties of Aggregates. Determination of Particle Size Distribution. Sieving Method; European Committee for Standardization, Brussels, Belgium, **2012**.
4. EN 1015-3: Methods of Test for Mortar for Masonry. Determination of Consistence of Fresh Mortar (by Flow Table); European Committee for Standardization, Brussels, Belgium, **1999**.
5. EN 1015-10: Methods of test for mortar for masonry – Part 10: Determination of dry bulk density of hardened mortar; European Committee for Standardization, Brussels, **1999**.
6. EN 1015-11: Methods of Test for Mortar for Masonry—Part 11: Determination of Flexural and Compressive Strength of Hardened Mortar; European Committee for Standardization, Brussels, Belgium, **1999**.
7. EN 1015-18: Methods of Test for Mortar for Masonry—Part 18: Determination of Water-Absorption Coefficient Due to Capillary Action of Hardened Mortar; European Committee for Standardization, Brussels, Belgium, **2002**.
8. EN 772-11: Methods of test for masonry units - Part 11: Determination of water absorption of aggregate concrete, manufactured stone and natural stone masonry units due to capillary action and the initial rate of water absorption of clay masonry units, European Committee for Standardization, Brussels, Belgium, **2000**.



© 2020 by the authors. Submitted for possible open access publication under the terms and conditions of the Creative Commons Attribution (CC BY) license (<http://creativecommons.org/licenses/by/4.0/>).